

MERCURY SORPTION ON CHITOSAN

K. Campos Gavilán, F. Peirano, J. Roussy, E. Guibal

Ecole des Mines d'Alès, Laboratoire Génie de l'Environnement Industriel,
6 avenue de Clavières, F-30319 Alès Cedex, France

Abstract

Mercury sorption on chitosan was investigated in batch and continuous systems. Preliminary experiments have been performed investigating the influence of pH on mercury sorption. Chitosan sorption properties were determined through sorption isotherms. Langmuir and Freundlich equations were used for the modelling of isotherms at pH 5. In batch systems, maximum sorption capacities reached 550 mg Hg/g. Sorption kinetics have been studied as a function of sorbent particle size and stirring rate. Simple models were used to determine the diffusion coefficients (intraparticle and external diffusion). Dynamic removal of mercury was tested in a fixed bed reactor investigating the following parameters: particle size, column size, flow velocity and metal ion concentration. Several simplified models have been verified for the simulation of breakthrough curves. This study shows that chitosan is an effective sorbent for the treatment and recovery of mercury from dilute effluents.

Key words: adsorption, chitosan, mercury ions, column size effect, concentration effect, fixed bed reactor, flow velocity effect particle size effect.

Introduction

The discharge of wastewaters from paper, pulp, oil refinery, chlor-alkali, pharmaceutical and battery manufacturing industry, presents an ongoing and serious threat to human health and natural water quality, mercury is considered by the Environmental Protection Agency (EPA) as a highly dangerous element because of its accumulative and persistent character in the environment and biota [1]. The necessity to reduce the amount of mercury ions in wastewater streams of industries, has led to an increasing interest in selective adsorbents: chitosan, alginate, etc. [2, 3].

Biosorption is a technique that uses waste biomass or natural biopolymers (low-cost materials) to sequester heavy metal ions from aqueous, it usually comprises several mechanisms: adsorption, ion exchange, chelation, micro-precipitation, etc. This alternative process is competitive, effective and cheap [4].

Chitosan can be extracted from chitin, the most abundant biopolymer in nature after cellulose, chitin is one of the principal components of crustacean shells. Chitosan is a linear polymer of D-glucosamine and contains high contents of amino and hydroxyl functional groups.

Chitosan has been reported for the high potentials of the adsorption metal ions (it contains a large number of free amine groups that are very reactive for chelation of metal cations in the near-neutral pH range) [5, 6]. Other useful features of chitosan include its abundance, non-toxicity, hydrophilicity, biocompatibility, biodegradability, and antibacterial property. [7]

The objective of the present work is to investigate the adsorption of mercury from aqueous solution by chitosan using batch and continuous system. In batch system the uptake capacity, pH, equilibrium and kinetics, were investigated, the equilibrium was well described by Langmuir and Freundlich biosorption isotherms and kinetics was well described by the equation of Weber and Morris; Spahn and Schlunder. In the case of fixed-bed systems the effects of design parameters such as bed height, flow rate, particle size, and metal initial concentration, have been investigated. The breakthrough profiles for the sorption of mercury in continuous system were analysed using Clark, and Adams-Bohart model.

Material and Methods

Biosorbent and chemicals

Chitosan was supplied by Mahtani Chitosan PVT. LTD. (Inde) as a flaked material, with a deacetylation percentage of about 87%, and a molecular weight close to 125,000 g/mol. Analytical grade reagents (HgCl₂, H₂SO₄, NaCl, NaOH) were used for the preparation of aqueous solution.

Batch experiments

Isotherms were performed by mixing a given amount of chitosan (10-50 mg) with 150 mL of mercury solution (concentration varying between 10 and 150 mg/L). The flasks were agitated at 500 rpm on a reciprocal shaker (Janke & Kunkel HS501 digital IKA LABORTECHNIK). The initial solution pH was adjusted using H₂SO₄ and NaOH at optimal pH (pH = 5). After 72 h of contact time, the chitosan was separated from metal solution by filtration. The metal content in the supernatant was determined using ICP-AES (inductively coupled plasma atomic emission spectrometry Jobin Yvon JY 2000, France).

The amount of metal adsorbed on chitosan was calculated using the mass balance equation:

$$q = \frac{V(C_o - C_{eq})}{M} \quad (1)$$

where q is the metal uptake (mg/g), C_o and C_{eq} the initial and equilibrium metal concentrations in the solution (mg/L) respectively; V the solution volume (L); and M the mass of biosorbent (g).

The equilibrium data were modelled using the Langmuir and Freundlich isotherm equations.

Langmuir equation:

$$q = q_m \frac{bC_{eq}}{1+bC_{eq}} \quad (2)$$

where C_{eq} and q show the residual metal concentration and the amount of metal adsorbed on the adsorbent at equilibrium, respectively, b is the Langmuir constant. [8]

Freundlich equation:

$$q = K_F C_{eq}^{\frac{1}{n}} \quad (3)$$

K_F , n are the constants of the Freundlich isotherm. [9]

kinetics studies

The effect of the time of exposure of the chitosan to mercury on the biosorption characteristics was investigated. The study of kinetics allow determine the required time for reaching the equilibrium and to identify the contribution of limiting steps (diffusion mechanisms).

The kinetics were performed at different agitation speeds 200, 350, and 500 rpm and different particle sizes G1 < 125 < G2 < 250 < G3 < 355.

There are different models for describing the kinetics of adsorption. The application of these models allows determining the coefficient of intraparticle diffusion and external diffusion.

Two simplified models are frequently used for describing kinetics of adsorption: Morris and Weber for intraparticle diffusion and Spahn and Schlunder for external diffusion.

Weber and Morris [10]:

$$q_t = Kt^{1/2} \quad (4)$$

where q_t (mg/g) is the amount of mercury adsorbed at time t , K the intraparticle rate constant ($\text{mg/g} \cdot \text{min}^{1/2}$).

Spahn and Schlunder

The variation of the concentration of solute in liquid phase follows the equation [11]:

$$V \frac{dC_{(t)}}{dt} = -k_f A (C_{(t)} - C_{SL(t)}) \quad (5)$$

where:

V : solution volume (L)

A : surface of exchange concerned by the external diffusion (m^2)

k_f : external diffusion coefficient ($\text{m} \cdot \text{min}^{-1}$)

C_{SL} : metal ion concentration on the interface solid-liquid ($\text{mg} \cdot \text{L}^{-1}$).

Column experiments

Continuous-flow sorption experiments were conducted in a glass column with internal diameter of 7 mm and different lengths. Since the ratio of column diameter to particle diameter is high, the effects of channelling are negligible. Glass beads (2 mm in diameter) were placed at the top of the column in order to provide a uniform flow. The experiments were carried out to study the effect of the following important variables at optimal pH (pH=5) such as: bed height 4.6-14.2 cm, flow rate of mercury solution 0.64-1.9 mL/min (giving a linear flow rate U_0 between 1-3 $\text{m} \cdot \text{h}^{-1}$), concentration of mercury solution 25-75 ppm, chitosan particle size 125-500 μm . The mass of sorbent was set at 0.5, 1 and 1.5 g (corresponding to depths Z of 4.6, 9.2 and 14.2 cm respectively, G2). The solution was pumped upflow at varying volumetric flow rate 0.64-1.9 mL/min. The effluent samples were taken at different intervals. The schematic diagram for the experimental set up is outlined in Figure 1.

The results were modelled using the Adams-Bohart model and the Clark model, Adams-Bohart modelling assumes that the adsorption rate is proportional to both the residual capacity of chitosan and the concentration of the solute species. Solving the different mass transfer equation and equilibrium constant leads to the following equation [12]:

$$\ln \left[\frac{C_0}{C} - 1 \right] = \frac{K_{AB} N_0 Z}{U_0} - k_{BA} C_0 t \quad (6)$$

where C is the effluent concentration ($\text{mg} \cdot \text{L}^{-1}$), C_0 the influent concentration ($\text{mg} \cdot \text{L}^{-1}$), K_{AB} the sorption rate coefficient ($\text{L} \cdot \text{mg}^{-1} \cdot \text{h}^{-1}$), N_0 the sorption capacity ($\text{mg} \cdot \text{L}^{-1}$), Z the bed height (mm), U_0 the linear velocity ($\text{mm} \cdot \text{h}^{-1}$) and t is the time (h). K_{AB} and N_0 the parameters of the equation can be obtained by linearization of $\ln [(C_0/C)-1]$ in function of t for C/C_0 below 0.15 at given column depths (Z).

Clark modelling associates the Freundlich equation and the mass transfer concept [13]:

$$\left(\frac{C_0}{C} \right)^{n-1} - 1 = A e^{-rt} \quad (7)$$

where n is the Freundlich parameter, K_c is the mass transfer coefficient (h^{-1}), and A and r are the Clark constants:

$$A = \exp \left(\frac{K_c N_0 Z}{U_0} \right) \text{ and} \quad (8)$$

$$r = K_c C_0 \quad (9)$$

linearizing Eq. (7)

$$\ln \left[\left(\frac{C_o}{C} \right)^{n-1} - 1 \right] = \ln A - rt \quad (10)$$

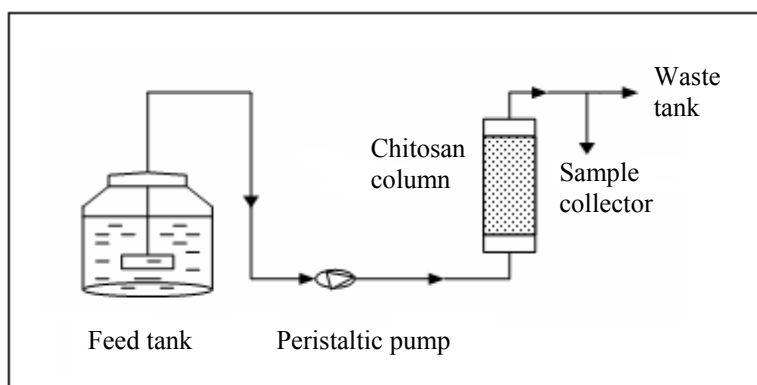


Figure 1 : Fixed-Bed system: Schematic diagram of experimental set up.

Results and discussion

Batch system

Sorption isotherms of Hg(II) cations. The isotherms are used to characterize the interactions of metal ions with the biosorbent. This provides a relationship between the concentration of metal ions in the sorption equilibrium in the sorption medium and the amount of metal ions adsorbed on the solid-phase at equilibrium. The adsorption isotherm and linearized Langmuir and Freundlich adsorption isotherms are illustrated in Figure 2, the values obtained for the respective constants are shown in Table 1 and Table 2. The Langmuir isotherm equation ($r^2=0.99$) fitted better the adsorption process of Hg (II) by chitosan than the Freundlich equation ($r^2=0.96$). In the Freundlich model when n is greater than 1 the sorption is considered “favorable”.

Table 1. Langmuir constants for Hg (II) sorption by chitosan after 72 h at 20° C and pH=5.

Langmuir Model	q_m (mg/g)	b (L/mg)	r^2
Weber linearization: $\frac{1}{q} = \frac{1}{q_m} + \frac{1}{q_m b C_{eq}}$	647	0.04	0.99
Stumn and Morgan linearization: $\frac{C_{eq}}{q} = \frac{1}{q_m b} + \frac{C_{eq}}{q_m}$	574	0.05	0.99

Table 2. Freundlich constants for Hg (II) sorption by chitosan after 72 h at 20° C and pH=5.

Freundlich Model	n	K_F (mg/g)	r^2
linearization: $\log q = \log K_F + \frac{1}{n} \log C_{eq}$	1.5	35.7	0.96

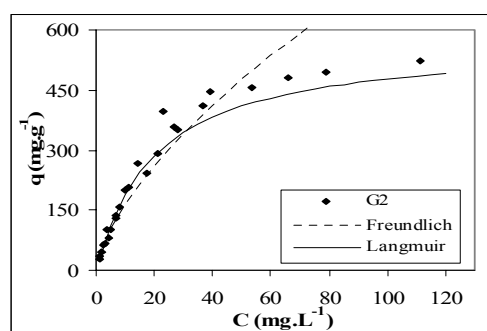


Figure 2 : Mercury adsorption isotherm (pH=5, T=20°C, particle size G2).

Sorption kinetics of Hg(II) cations. Sorption kinetics are generally controlled by different diffusion mechanisms such as external and intraparticle diffusion. In order to evaluate the contribution of external diffusion the velocity of agitation was varied between 200 and 500 rpm. Figure 3 a) shows that increasing agitation speed improves sorption rate (above 350 rpm the sorption kinetics stabilizes). When increasing the agitation speed, the diffusion rate of mercury ions from the bulk liquid to the liquid boundary layer surrounding particles became higher because of an enhancement of turbulence and a decrease of the thickness of the boundary layer. For measuring the impact of intraparticle diffusion it is common to investigate the influence of particle size on kinetic profiles and sorption isotherms. Figure 3 b) shows that the kinetics curves overlay for particles G1, G2, and G3. Intraparticle diffusion is not the main limiting step. When sorption is controlled by intraparticle diffusion, as a consequence of poor porosity the equilibrium sorption can be also decreased with increasing the particle size (sorption being restricted to the external surface). This is not the case for Hg binding on chitosan. Table 3 shows that the intraparticle diffusion coefficient slightly decreases with increasing particle size. Considering the Spahn and Schlunder model (i. e. external diffusion model) the variation is not continuous with particle size variation. The parameters obtained from the Spahn and Schlunder model and Weber –Morris model are shown in Table 3.

Table 3. The parameters obtained from the Spahn and Schlunder model and Weber –Morris model for Hg (II) biosorption.

parameter	Spahn and Schlunder model			Weber and Morris model	
	External diffusion			Intraparticle diffusion	
	$K_f A/V(\text{min}^{-1})$	$K_f(\text{mm}.\text{min}^{-1})$	r^2	$K_w(\text{mg}.\text{L}^{-1}.\text{s}^{-0.5})$	r^2
G1	0.060	1.6×10^{-3}	0.96	21.9	0.96
G2	0.034	3.0×10^{-4}	0.98	18.0	0.99
G3	0.023	1.2×10^{-4}	0.97	13.4	0.98
200 rpm	0.020	1.7×10^{-4}	0.97	10.4	0.99
350 rpm	0.034	3.0×10^{-4}	0.98	18.0	0.99
500 rpm	0.036	3.1×10^{-4}	0.98	17.2	0.99

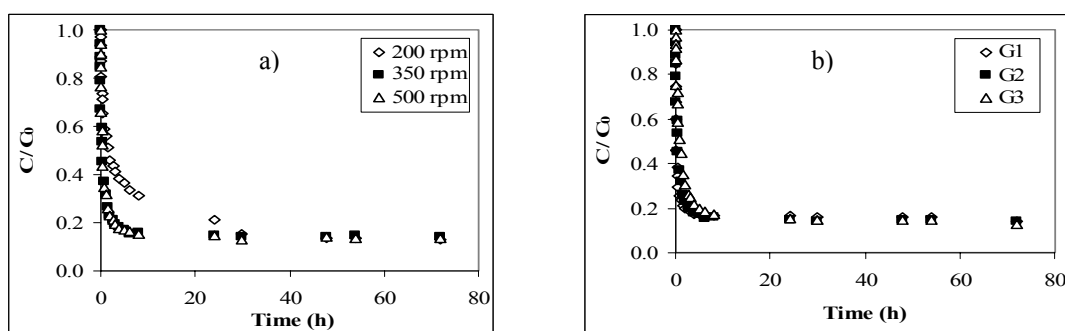


Figure 3 : a) Effect of agitation speed on kinetics (pH=5, mercury solution 50 mg/L, Chitosan solution 300 mg/L). b) Effect of chitosan particle on kinetics (pH=5, mercury solution 50 mg/L, Chitosan solution 300 mg/L).

Fixed-bed systems

The simulated breakthrough curves are given in Figure 4. Adams-Bohart model was applied to experimental data for the description of the initial part of the breakthrough curve ($C/C_0 < 0.15$), this approach was focused on the estimation of characteristic parameters, such as maximum adsorption capacity (N_0) and kinetic constant (K_{AB}). Sorption capacity of the chitosan increases with increasing the depth, initial concentration, flow rate, but in the case of particle size, lower size particles are more favorable for mercury uptake but the pressure drop increases with decrease in the particle size.

In the fixed bed column, Freundlich constants n (determined in previous section) were used to calculate the parameters in the Clark model; the parameters of the Clark and Adams-Bohart equation are given in Table 4. The Clark model fit well the experimental results, but the initial part of the breakthrough curve was not defined; Aksu [13] and Hamdaoui [14] obtained that at ratios $C/C_0 < 0.07$ the model could not applied to experimental data.

Table 4. The parameters obtained from Adams-Bohart and Clark model.

parameter	Adams-Bohart model			Clark model		
	$N_0 \times 10^5$ (mg/L)	$K_{AB} \times 10^{-3}$ (L/mg.h)	r^2	$\ln A$	$rx10^{-2}$	r^2
Z=4.6 cm	1.08	6.0	0.96	1.21	0.06	0.95
Z=9.2 cm	1.35	4.4	0.99	3.35	0.06	0.97
Z=14.2 cm	1.53	1.8	0.97	3.40	0.04	0.96
Co=25 ppm	0.63	6.3	0.98	0.84	0.03	0.97
Co=50 ppm	0.82	5.4	0.95	2.96	0.07	0.97
Co=100 ppm	1.06	3.7	0.99	1.83	0.12	0.99
Uo=1 m/h	0.79	2.4	0.97	0.80	0.03	0.93
Uo=2 m/h	0.82	5.4	0.95	2.96	0.07	0.97
Uo=3 m/h	0.85	6.1	0.99	1.15	0.10	0.99
G 2	1.08	6.0	0.96	1.21	0.06	0.95
G 3	0.82	5.4	0.95	2.96	0.07	0.97
G 4	0.58	2.0	< 0.9	0.03	0.04	0.96

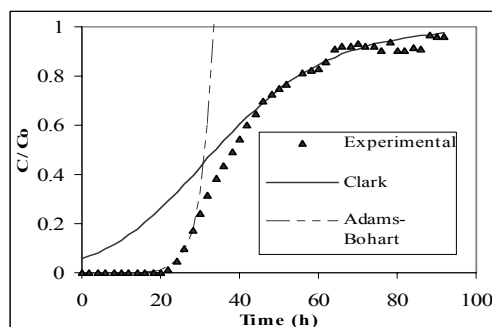


Figure 4 : The breakthrough curve of Hg (II) sorption by chitosan with Adams-Bohart and Clark model. ($C_0=50$ ppm, $v=1.9$ mL/min, $Z=6.1$ cm, particle size G3).

Effect of depth. Breakthrough time and exhaustion time increase linearly with column depths (Figure 5 a). N_0 , which correlates to the sorption capacity, increases with increasing the depth of the column. Increasing the depth of the columns increase the residence time, which facilitated the saturation of the sorbent.

Effect of metal concentration. In Figure 5 b) shows the breakthrough profiles for the adsorption of mercury at different initial concentrations. With decreasing the inlet Hg (II) concentration the breakthrough curves were delayed and the treated volume increased at breakthrough. Lower concentration gradient caused slower transport due to decreased diffusion coefficient, or decreased mass transfer coefficient.

Effect of flow rate. In Figure 6 a) breakthrough and exhaustion occurred faster at higher flow rates. Also as the flow rate increases, metal concentration in the effluent increased rapidly resulting in much sharper breakthrough curves. This behaviour may be due to insufficient residence time of the solute in the column and to diffusion limitations.

Effect of particle size. Figure 6 b) shows that particle size has a limited impact on the breakthrough curves. The curves almost overlap, indicating that intraparticle diffusion does not control the dynamic sorption of mercury on chitosan. This result is consistent with those obtained in batch (Figure 3 b). However Table 4 shows that maximum sorption capacity decreases with increasing particle size, based on Adams-Bohart equation which only models the beginning of the breakthrough curve.

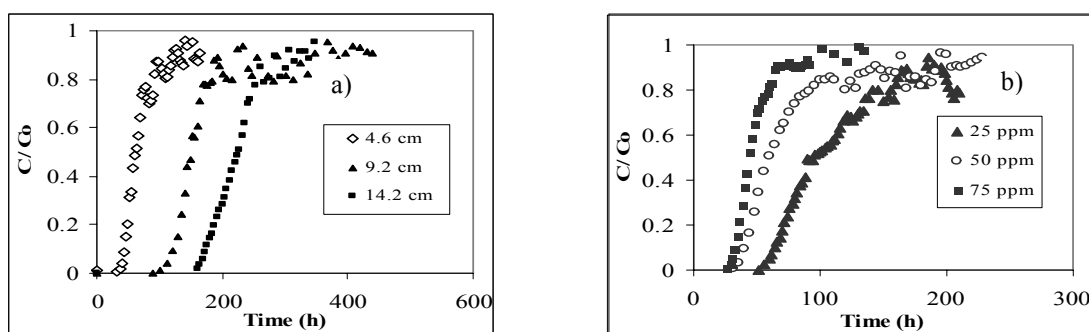


Figure 5 : a)Effect of bed height ($C_0= 50$ ppm, $v=1,28$ ml/min, particle size G2, $pH=5$). b)Effect of metal concentration ($v=1,28$ ml/min, $Z=6,2$ cm, particle size G3, $pH=5$).

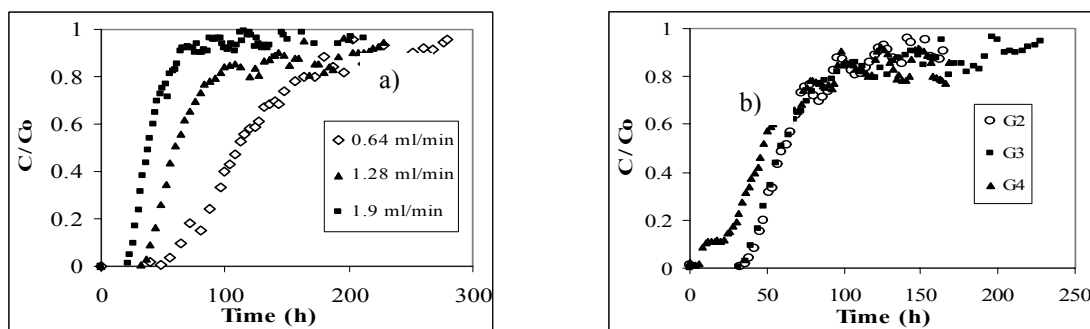


Figure 6 : a) Effect of flow rate ($C_0=50$ ppm, $Z= 6$ cm, particle size G3, $pH=5$). b) Effect of particle size ($C_0=50$ ppm, $v=1.28$ ml/min).

Conclusions:

On the basis of the present study, the following conclusions can be drawn:

The sorption isotherms show that the Langmuir equation is the best predicting model for the simulation of experimental data. The uptake of mercury by chitosan can reach up to 550 g/Kg. The adsorption process depends of different factors as particle size, chitosan dosage, metal concentration. The kinetics data show that increasing agitation speed improves sorption rate but above 350 rpm, the sorption kinetics stabilizes.

The intraparticle diffusion was not the main limiting step. Both external and intraparticle diffusion mechanism contribute to kinetic control.

Adams-Bohart and Clark models were applied to experimental data obtained from fixed-bed system, these models gave good approximations of experimental behavior.

Mercury ions adsorbed on chitosan columns were desorbed effectively about 80% by H_2SO_4 0.5 M (work in progress).

Acknowledgements:

Karol Campos Gavilán thanks the support from Raul Porras Barrenechea program for collaboration Franco-Peruvian.

Reference

- [1] K. Graeme, C. Pollack, J. Emerg.. Med. 16.1 (1998) 45-56.
- [2] Y. Kawamura, H. Yoshida, S. Asai and H. Tanibe. J. Chem. Eng. Japan 31.1(1998) 1-6.
- [3] Y. Yacar, C. Arpa, S. Tan, A. Denizli Process Biochem. 37.(2002) 601-610.
- [4] D. Volesky, A. Mucci. Wat. Res. 37 (2003) 4311-4330.
- [5] E. Guibal, Sep. Purif. Tech 38 (2004) 43-74.
- [6] R. Juang, F. Wu and R. Tseng. Wat. Res. 33.10 (1999) 2403-2409.
- [7] R. Kumar React. Funct. Polym. 46 (2000) 1-27.
- [8] I. Safarik Wat. Res. 29.1 (1995) 101-105.
- [9] Y. Kacar, C. Arpa, S. Tan, A. Denizli, O. Genc. Process Biochem. 37 (2002) 601-610.
- [10] A.Ozer, G. Akkaya, and M. Turabik J. Hazard. Mater. B126 (2005) 119-127.
- [11] P. Chassary Ph. D. project. Montpellier university (2004).
- [12] H. Tran and F. Roddick Wat. Res. 33.13 (1999) 3001-3011.

- [13] Z. Aksu and F. Gonen *Process Biochem.* 39 (2004) 599-613.
- [14] O. Hamdaoui *J. Hazard. Mater.* 2006.